Development and Application of a Fast Multipole Method in a Hybrid FEM/MoM Field Solver

Chunlei Guo and Todd H. Hubing
Department of Electrical and Computer Engineering
University of Missouri-Rolla
Rolla, MO 65409

ABSTRACT

Hybrid FEM/MoM methods combine the finite element method (FEM) and the method of moments (MoM) to model inhomogeneous unbounded problems. These two methods are coupled by enforcing the continuity of tangential fields on the boundary that separates the FEM and MoM regions. When modeling complex geometries with many elements on the boundary, the MoM part of the problem is the bottleneck of the hybrid method since it requires $O(N^2)$ memory and $O(N^3)$ computation time. This paper presents a hybrid FEM/MoM formulation applying the fast multipole method (FMM) that greatly reduces the memory requirement associated with MoM part. Two practical electromagnetic problems are presented to validate this method.

INTRODUCTION

The hybrid finite-element-method/method-of-moments (FEM/MoM) has been used to analyze a variety of electromagnetic scattering and radiation problems effectively. FEM is used to model detailed structures with complex inhomogeneities and MoM is used to model larger metallic structures and to provide an exact radiation boundary condition to terminate the FEM mesh. These two methods are coupled by enforcing tangential field continuity on the boundary separating the FEM and MoM regions. Both the FEM and MoM are powerful methods, but each of these methods has its own advantages and disadvantages. MoM handles unbounded problems very effectively but is less efficient when complex inhomogeneities are present. Inhomogeneities are easily handled by FEM. However, FEM is most suitable for bounded problems. Hence, methods that combine MoM and FEM are advantageous for treating electromagnetic problems involving unbounded, complex structures.

The FEM part of the hybrid method produces a sparse matrix, which requires $O(N)$ memory, where N is the total number of unknowns in the FEM region. On the other hand, the MoM part of the hybrid method produces a dense matrix, which requires $O(N_S^2)$ memory and $O(N_S^3)$ CPU time, where N_S is the total number of unknowns on the MoM boundary. The final system of equations produced by the hybrid method consists of a partially full, partially sparse matrix. An iterative solver is usually preferred to solve this matrix equation. However, the computational effort primarily associated with the MoM part limits the size of the problems that can be solved.

Rokhlin introduced a fast multipole method to speed up the matrix-vector multiplication that arises in the iterative solution of MoM equations [1]. This method has been applied to electromagnetic scattering computation by Engheta [2], Lu [3], and Song [4] *et al*. The memory required for matrix-vector multiplications can be reduced from $O(N_S^2)$ in MoM to $O(N_S^{1.5})$ by using a two-level FMM, and to $O(N_S \log N_S)$ by using a multilevel version of the FMM method.

In this paper, a two-level FMM is implemented in a hybrid FEM/MoM method. Section II describes the formulation of the hybrid FEM/MoM and the related formulation using the FMM method. Preconditioning techniques to improve the condition of the resulting system of equations are also discussed. Section III presents numerical results using the FMM-enhanced hybrid FEM/MoM method.

FORMULATION

The FMM method provides an efficient technique for performing matrix-vector multiplications for MoM matrices. This section describes the hybrid FEM/MoM formulation with FMM applied to the evaluation of the MoM integrals.

The Hybrid FEM/MoM Formulation

In the hybrid FEM/MoM, an electromagnetic problem is divided into an interior equivalent part and an exterior equivalent part. The interior part is modeled using the FEM and the exterior part is

modeled using a surface integral equation method. The two equivalent parts are coupled by enforcing the continuity of tangential fields on the FEM and MoM boundaries [5].

FEM is used to analyze the interior equivalent part by solving the weak form of the vector wave equation [6]:

$$\int_V \left[\left(\frac{\nabla \times \mathbf{E(r)}}{j\omega\mu_0\mu_r} \right) \bullet \left(\nabla \times \mathbf{w(r)} + j\,\omega\,\varepsilon_0\varepsilon_r \mathbf{E(r)} \bullet \mathbf{w(r)} \right) \right] dV = \int_S \left(\hat{n} \times \mathbf{H(r)} \right) \bullet \mathbf{w(r)}\, dS - \int_V \mathbf{J}^{\text{int}}(\mathbf{r}) \bullet \mathbf{w(r)}\, dV \tag{1}$$

where S is the surface enclosing volume V, $\mathbf{w(r)}$ is the weighting function, and $\mathbf{J}^{\text{int}}$ is an impressed source inside volume V. A Galerkin procedure is usually used to test equation (1). The resulting FEM matrix equation has the form,

$$\begin{bmatrix} A_{ii} & A_{is} \\ A_{si} & A_{ss} \end{bmatrix} \begin{bmatrix} E_i \\ E_s \end{bmatrix} = \begin{bmatrix} 0 & 0 \\ 0 & B_{ss} \end{bmatrix} \begin{bmatrix} 0 \\ J_s \end{bmatrix} + \begin{bmatrix} g_i \\ g_s \end{bmatrix} \tag{2}$$

where $\{E_i\}$ is a set of unknowns for the electric field within the FEM volume; $\{E_s\}$ and $\{J_s\}$ are sets of unknowns for the electric field and the electric current density on the dielectric surface, respectively; A_{ii}, A_{is}, A_{si}, A_{ss} and B_{ss} are sparse coefficient matrices; and g_i and g_s are source terms.

The exterior equivalent problem can be analyzed by using an electric field integral equation (EFIE), magnetic field integral equation (MFIE), or both, i.e., combined field integral equation (CFIE). Both the EFIE and MFIE equations are prone to errors at frequencies corresponding to the resonant frequencies of the closed surface. However, proper formulation of the CFIE is free of such errors [6]. The EFIE is in the form [7],

$$\begin{aligned} \mathbf{E}^{\text{inc}}(\mathbf{r}) = \frac{1}{2}\mathbf{E}(\mathbf{r}) + \int_S \Big[& \mathbf{M}(\mathbf{r}') \times \nabla' \mathrm{G}_0(\mathbf{r},\mathbf{r}') \\ & + jk_0\eta_0 \mathbf{J}(\mathbf{r}')\,\mathrm{G}_0(\mathbf{r},\mathbf{r}') \\ & - j\frac{\eta_0}{k_0} \nabla' \bullet \mathbf{J}(\mathbf{r}') \nabla' \mathrm{G}_0(\mathbf{r},\mathbf{r}') \Big] dS', \quad \mathbf{r} \in S \end{aligned} \tag{3}$$

where k_0 and η_0 are the wavenumber and the intrinsic wave impedance in free-space. The MFIE is the dual of the EFIE [7],

$$\begin{aligned} \mathbf{H}^{\text{inc}}(\mathbf{r}) = \frac{1}{2}\mathbf{H}(\mathbf{r}) + \int_S \Big[& -\mathbf{J}(\mathbf{r}') \times \nabla' \mathrm{G}_0(\mathbf{r},\mathbf{r}') \\ & + j\frac{k_0}{\eta_0} \mathbf{M}(\mathbf{r}')\,\mathrm{G}_0(\mathbf{r},\mathbf{r}') \\ & - j\frac{1}{k_0\eta_0} \nabla' \bullet \mathbf{M}(\mathbf{r}') \nabla' \mathrm{G}_0(\mathbf{r},\mathbf{r}') \Big] dS', \quad \mathbf{r} \in S. \end{aligned} \tag{4}$$

The integral term in equations (3) and (4) is a principal-value integral, i.e., the singularity at $\mathbf{r} = \mathbf{r}'$ is excluded.

The equivalent currents on the boundary are represented by a series of basis functions. In this case, triangular basis functions, $\mathbf{f}(\mathbf{r})$, (RWG basis functions) were employed [8],

$$\mathbf{J}(\mathbf{r}) = \sum_{n=1}^{N_s} (J_s)\mathbf{f}_n(\mathbf{r}) \tag{5}$$

$$\mathbf{M}(\mathbf{r}) = \sum_{n=1}^{N_s} (E_s)\mathbf{f}_n(\mathbf{r}) \tag{6}$$

where N_s is the total number of unknowns on the surface S. The EFIE and MFIE in equations (3) and (4) have four different discrete forms using different testing functions [9]. Two of them, TE and NE, are described in the following sections. In both cases, the resulting MoM matrix equation has the following structure,

$$[C]\ [J_s] = [D]\ [E_s] - [F]. \tag{7}$$

The TE form

One method of discretizing the EFIE is known as the TE form (short for $\hat{t} \cdot \boldsymbol{E}$ where $\hat{t}$ denotes a unit vector tangential to S). In this form, the EFIE in Equation (3) is tested using functions $\mathbf{f}(\mathbf{r})$. The elements in matrices [C], [D] and [F] are then given by [10],

$$\begin{aligned} C_{mn} = & -jk_0\eta_0 \int_{S_m} \mathbf{f}_m(\mathbf{r}) \bullet \left[\int_{S_n} \mathbf{f}_n(\mathbf{r}')\,\mathrm{G}_0(\mathbf{r},\mathbf{r}')\, dS' \right] dS \\ & + j\frac{\eta_0}{k_0} \int_{S_m} \nabla \bullet \mathbf{f}_m(\mathbf{r}) \left[\int_{S_n} \left(\nabla' \bullet \mathbf{f}_n(\mathbf{r}') \right) \mathrm{G}_0(\mathbf{r},\mathbf{r}')\, dS' \right] dS \end{aligned} \tag{8}$$

$$D_{mn} = \int_{S_m} \mathbf{f}_m(\mathbf{r}) \bullet \left[\int_{S_n} \mathbf{f}_n(\mathbf{r}') \times \nabla' \mathrm{G}_0(\mathbf{r},\mathbf{r}')\, dS' + \frac{1}{2}\,\mathbf{w}_n(\mathbf{r}) \right] dS \tag{9}$$

$$F_m = \int_{S_m} \mathbf{f}_m(\mathbf{r}) \bullet\ \mathbf{E}^{\text{inc}}(\mathbf{r})\, dS. \tag{10}$$

In equation (8), the ∇ operator has been transferred to the testing function $\mathbf{f}_m(\mathbf{r})$ so that C_{mn} has an R^{-1} singularity that can be evaluated analytically [8].

The NE form

In this form, the EFIE in Equation (3) is tested using functions $\hat{\mathbf{n}} \times \mathbf{f(r)}$, where $\hat{n}$ is a unit normal vector pointing outward from the boundary surface. The elements in the matrices [*C*], [*D*] and [*F*] are given by [10],

$$C_{mn} = -jk_0\eta_0 \int_{S_m} \mathbf{f}_m(\mathbf{r}) \bullet \left[\hat{n} \times \int_{S_n} \mathbf{f}_n(\mathbf{r}') \, \mathrm{G}_0(\mathbf{r},\mathbf{r}') dS' \right] dS + j\frac{\eta_0}{k_0} \int_{S_m} \mathbf{f}_m(\mathbf{r}) \bullet \left[\hat{n} \times \int_{S_n} \left(\nabla' \bullet \mathbf{f}_n(\mathbf{r}') \right) \nabla' \mathrm{G}_0(\mathbf{r},\mathbf{r}') dS' \right] dS \tag{11}$$

$$D_{mn} = \int_{S_m} \mathbf{f}_m(\mathbf{r}) \bullet \left[\hat{n} \times \int_{S_n} \mathbf{f}_n(\mathbf{r}') \times \nabla' \mathrm{G}_0(\mathbf{r},\mathbf{r}') dS' - \frac{1}{2}\mathbf{f}_n(\mathbf{r}) \right] dS \tag{12}$$

$$F_m = \int_{S_m} \mathbf{f}_m(\mathbf{r}) \bullet \left[\hat{n} \times \mathbf{E}^{\mathrm{inc}}(\mathbf{r}) \right] dS. \tag{13}$$

The matrix elements in TH and NH forms can be derived from those in TE and NE forms.

Note that neither the FEM matrix equation (2) nor the MoM matrix equation (7) can be solved independently. They are coupled through the J_s and E_s terms. Three different formulations, the combined formulation, the inward-looking formulation and the outward-looking formulation, can be used to solve the coupled system [6], [13].

Application of the FMM Method

To apply the FMM, the N_s basis functions are divided into *M* localized groups, labeled by an index *l*, each supporting N_s/M basis functions. For nearby group pairs (l,l'), the matrix elements are calculated using the numerical evaluation of equations (8)–(13). For non-nearby groups (l,l'), let $\mathbf{r}_m$ be the observation point, $\mathbf{r}_n$ be the source point, $\mathbf{r}_l$ be the center of *l* group which contains $\mathbf{r}_m$, and $\mathbf{r}_{l'}$ is the center of l' group which contains $\mathbf{r}_n$,

$$\begin{aligned} \mathbf{r}_{mn} &= \mathbf{r}_m - \mathbf{r}_n \\ &= \mathbf{r}_m - \mathbf{r}_l + \mathbf{r}_l - \mathbf{r}_{l'} + \mathbf{r}_{l'} - \mathbf{r}_n \\ &= \mathbf{r}_{ll'} + \mathbf{r}_{ml} - \mathbf{r}_{nl'}. \end{aligned} \tag{14}$$

For simplicity, the same subscripts used to label basis functions are employed to label the source and observation points here. Equation (14) breaks the path from the source point $\mathbf{r}_n$ to the observation point $\mathbf{r}_m$ into three parts: the path from the source point to the center of the l' group, the path from the center of the l' group to the center of the *l* group, and the path from the center of the *l* group to the observation point. The scalar Green's function between the source point and the observation point can be approximated as [3],

$$\begin{aligned} \mathrm{G}_0(\mathbf{r}_m,\mathbf{r}_n) &= \frac{e^{-jk_0 r_{mn}}}{4\pi r_{mn}} \\ &\approx \frac{-jk_0}{16\pi^2} \oint e^{-jk_0(\mathbf{r}_{ml}-\mathbf{r}_{nl'})} \mathrm{T}_L\left(k_0 r_{ll'}, \hat{k} \bullet \hat{r}_{ll'}\right) d^2\hat{k} \end{aligned} \tag{15}$$

where $\oint d^2\hat{k}$ is a surface integral over a unit sphere, and

$$\mathrm{T}_L(\kappa, \cos\theta) = \sum_{l=0}^{L} (-j)^l (2l+1) h_l^{(2)}(\kappa) P_l(\cos\theta) \tag{16}$$

where $h_l^{(2)}(x)$ is a spherical Hankel function of the second kind and $P_l(x)$ is a Legendre polynomial.

Substituting (15) into equations (8), (9), (11), and (12), we can get the matrix elements in TE and TH form using the approximate Green's function. These elements seem to be more complicated than their counterparts obtained using the MoM method, but they can be evaluated more efficiently.

The TE form

The elements in matrices [*C*] and [*D*] are approximated by,

$$\begin{aligned} C_{mn} = &-\left(\frac{k_0}{4\pi}\right)^2 \eta_0 \oint \mathbf{U}_{ml}^{C,TE} \bullet \mathrm{T}_L(k_0 r_{ll'}, \hat{k} \bullet \hat{r}_{ll'}) \mathbf{V}_{nl} d^2\hat{k} \\ &+ \frac{\eta_0}{(2\pi)^2} \oint U_{ml}^{C} \, \mathrm{T}_L(k_0 r_{ll'}, \hat{k} \bullet \hat{r}_{ll'}) V_{nl'} d^2\hat{k} \end{aligned} \tag{17}$$

$$D_{mn} = \left(\frac{k_0}{4\pi}\right)^2 \oint \mathbf{U}_{ml}^{D,TE} \bullet \mathrm{T}_L(k_0 r_{ll'}, \hat{k} \bullet \hat{r}_{ll'}) \mathbf{V}_{nl'} d^2\hat{k} \tag{18}$$

where

$$\mathbf{U}_{ml}^{C,TE} = \int_{S_m} e^{-j\mathbf{k}_0 \bullet \mathbf{r}_{ml}} \mathbf{f}_m(\mathbf{r}) dS \tag{19}$$

$$\mathbf{V}_{nl'} = \int_{S_n} e^{j\mathbf{k}_0 \bullet \mathbf{r}_{nl'}} \mathbf{f}_n(\mathbf{r}) dS \tag{20}$$

$$U_{ml}^{C} = \int_{S_m} e^{-j\mathbf{k}_0 \bullet \mathbf{r}_{ml}} dS \tag{21}$$

$$V_{nl'} = \int_{S_n} e^{j\mathbf{k}_0 \bullet \mathbf{r}_{nl'}} dS \tag{22}$$

$$\mathbf{U}_{ml}^{D,TE} = \hat{k} \times \mathbf{U}_{ml}^{C,TE} . \tag{23}$$

Equation (17) requires both a vector dot product of $\mathbf{U}_{ml}^{C}$ with $\mathbf{V}_{nl'}$ and a scalar product of U_{ml}^{C} with $V_{nl'}$.

The NE form

Similarly, the elements in matrices [*C*] and [*D*] in equations (11) and (12) are given by,

$$C_{mn} = \left(\frac{k_0}{4\pi}\right)^2 \eta_0 \oint\oint \mathbf{U}_{ml}^{C,NH} \bullet \mathrm{T}_L(k_0 r_{ll'}, \hat{k} \bullet \hat{r}_{ll'}) \mathbf{V}_{nl} d^2\hat{k} - \frac{j2k_0\eta_0}{(4\pi)^2} \oint\oint U_{ml}^{C,NH} \mathrm{T}_L(k_0 r_{ll'}, \hat{k} \bullet \hat{r}_{ll'}) V_{nl'} d^2\hat{k} \tag{24}$$

$$D_{mn} = \left(\frac{k_0}{4\pi}\right)^2 \oint\oint \mathbf{U}_{ml}^{D,NH} \bullet \mathrm{T}_L(k_0 r_{ll'}, \hat{k} \bullet \hat{r}_{ll'}) \mathbf{V}_{nl'} d^2\hat{k} \tag{25}$$

where

$$\mathbf{U}_{ml}^{C,NH} = \mathbf{U}_{ml}^{C,TE} \times \hat{n} \tag{26}$$

$$U_{ml}^{C,NH} = \hat{k} \bullet \mathbf{U}_{ml}^{C,NH} \tag{27}$$

$$\mathbf{U}_{ml}^{D,NH} = \hat{k} \times \mathbf{U}_{ml}^{C,NH} \tag{28}$$

Figure 1 illustrates how the computational complexity can be reduced by applying FMM, which applies approximate Green's functions to the evaluation of MoM integrals. In this figure, a hollow circle represents a source point, a solid circle represents an observation point, a hollow square represents a group center for a few source points, a solid square represents a group center for a few observation points, and a line that connects a circle with a circle or a square represents a matrix element resulting from the direct interaction from the two connecting objects. Using the MoM method, the four points illustrated in Fig. 1(a) generate a matrix with $4 \times 4 = 16$ elements. Using the FMM method however, every two points are grouped together, and only the group center has a one-to-one interaction with the other group centers. The matrix illustrated in Fig. 1(b) has only 12 elements since the number of one-to-one interactions is reduced. When there are more groups and more points per group, this reduction can be much more significant.

An iterative solver based on the inward-looking formulation or the combined formulation is usually preferred for the solution of the hybrid FEM/MoM matrix equation when the FMM method is employed. The combined formulation was used in this study since it doesn't require a direct inverse of the FEM matrix.

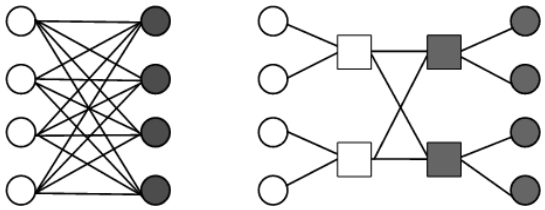

(a) MoM (b) FMM

Figure 1. Computational complexity reduction by using FMM.

The hybrid FEM/MoM matrix equation employing the combined formulation is given by,

$$\begin{bmatrix} A_{ii} & A_{is} & 0 \\ A_{si} & A_{ss} & -B_{ss} \\ 0 & D & -C \end{bmatrix} \begin{bmatrix} E_i \\ E_s \\ J_s \end{bmatrix} = \begin{bmatrix} g_i \\ g_s \\ F \end{bmatrix}. \tag{29}$$

In practice when the FMM method is employed, the *C* and *D* matrix elements resulting from far groups in equation (29) are not generated explicitly using equations (17), (18), (24), and (25). Instead, these equations are used to generate the matrix-vector multiplication directly [3]. So the explicit *C* and *D* matrices are sparse and contain only elements resulting from the nearby groups generated using the MoM method, denoted as C_{near} and D_{near}, respectively. Thus, the near matrix LHS' is given by

$$[LHS'] = \begin{bmatrix} A_{ii} & A_{is} & 0 \\ A_{si} & A_{ss} & -B_{ss} \\ 0 & D_{near} & -C_{near} \end{bmatrix}. \tag{30}$$

Preconditioning technique

The convergence of an iterative solution is strongly dependent on the condition of the matrix and the iterative solver used. The coefficient matrices generated by hybrid FEM/MoM techniques often have very large condition numbers. Without a preconditioner, the iterative solver may converge very slowly, or not at all. A good preconditioner should be easy to construct, require little memory and improve the convergence rate significantly.

Diagonal and block diagonal preconditioners have been widely used in the past [4]. LU and incomplete LU (ILU) factorization are commonly used to construct these preconditioners [15]. Matrix *LHS′* in equation (30) and the preconditioner LU matrices are usually the major memory consumers for an iterative solver. Special techniques must be applied to reduce the memory requirements of the preconditioner for electrically large problems [16].

In this study, a biconjugate gradient stabilized (BICGSTAB) solver was implemented. BICGSTAB is a popular and stable Krylov subspace method for the iterative solution of linear systems. A preconditioner using the absorbing boundary condition (ABC) to provide a physical approximation of the MoM boundary was also employed [17, 18].

NUMERICAL RESULTS

EMAP5 (Electromagnetic Analysis Program Version 5) is a hybrid FEM/MoM modeling code that has been used to model signal integrity, scattering and radiation problems [19]. On a personal computer with 1 GByte of memory, EMAP5 is generally limited to the solution of problems with no more than 3600 boundary elements. The fast multipole method described in the previous section was implemented in EMAP5 in order to model larger problems. This section describes two practical examples. A commercial mesh generator was used to discretize the problems presented in this paper. Results obtained from the FMM-enhanced EMAP5 (EMAP5-FMM) are compared to results obtained using other well-established codes or analytical results.

The first sample problem is to model the input impedance of a printed circuit board (PCB) power bus structure. As shown in Fig. 2, the board dimensions are 10 cm × 8 cm × 2 mm. The top and bottom planes are perfect electric conductors (PECs). The dielectric between the PEC layers has a relative dielectric constant of 4.2 and a loss tangent of 0.02. An ideal current source is used to excite the structure at the point ($x_i = 3$ cm, $y_i = 2$ cm). The frequency range of interest is from 30 MHz to 5 GHz.

The MoM boundary was chosen to be the physical boundary of the board. The mesh density used for this problem was 12 elements per wavelength at 5 GHz. The discretization of this problem is summarized in Table 1. The total number of unknowns is given by the sum of the number of E_i, E_d, J_h and J_c elements. The TE form is sufficient to generate a stable solution for this problem.

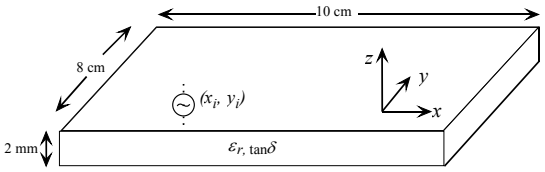

Figure 2. A PCB power bus structure.

In order to achieve a good approximation in equation (15), the size of a group should be proportional to the wavelength, so the number of groups varies with frequency. The number of groups generated for this structure at different frequencies is shown in Figure 3. At lower frequencies (e.g. below 1.5 GHz), the structure is electrically small, and the size of all groups must be much smaller than a wavelength. In this situation, the approximation in equation (15) becomes numerically unstable due to the divergent behavior of the spherical Hankel function when its order is much larger than its argument. It is invalid to use equation (15) in such cases, and all the elements must be in the same group (i.e., the matrix elements should be evaluated using MoM integrals). As the frequency increases, the wavelength decreases and the software assigns more groups to this structure. Figure 4 shows the groups of surface triangles at 5 GHz using different shades of gray to represent different groups. There are a total of 30 groups.

Table 1. Discretization of the problems

	Problem 1	Problem 2
Number of nodes	798	7,854
Number of tetrahedral elements	2,189	23,376
Number of triangles	1,580	9,186
Number of inner edges (E_i)	1,406	15,533
Number of FEM boundary edges (E_d)	144	13,779
Number of MoM boundary edges (J_h+J_c)	2,370	13,779
Total number of unknowns	3,920	43,091

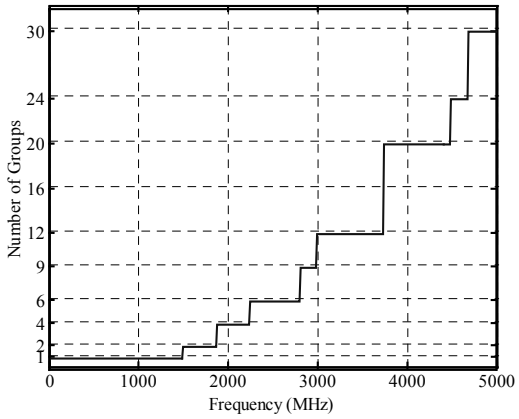

Figure 3. Number of groups at different frequecies for sample problem 1.

Groups (l,l') are defined as near groups when the following criteria are satisfied,

$$D = \left|\mathbf{r}_{ll'}\right| < 1.5 \max(d) \tag{39}$$

where D is the distance between two groups, max(d) is the maximum size of a group.

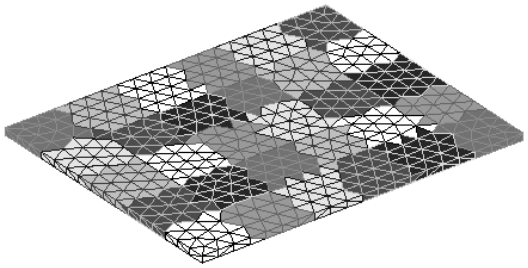

Figure 4. Mesh and groups for problem 1 at 5 GHz.

Since there are a total of 3920 unknowns in this structure, the near matrix *LHS'* in equation (30) can be used to build the preconditioner without exceeding the memory limit on a personal computer. Since the C and D matrices are dominated by the near group contributions evaluated using MoM, an ILU factorization on *LHS'* reduces the condition number of the matrix on the left hand side of equation (29) and the number of iterations significantly.

Figure 5 shows a plot of the memory required by *LHS'* and using ILU factorization on *LHS'* as a preconditioner. In this study, ILU factorization based on drop tolerance was adopted [15]. The memory required to evaluate equations (19), (20), (26), and (27) is negligible since no matrix elements are generated explicitly. The general behavior of the memory requirement versus frequency is directly related to the number of groups shown in Fig. 3. As frequency goes up, there are more groups, and more interactions between group pairs may be evaluated using the FMM method, thus the memory required to store the near matrix is reduced. Below 2.8 GHz, although the number of groups varies from 1 to 9, the groups are so close to each other that the interaction between them has to be evaluated by the MoM integrals, so the memory required to store the near matrix is about the same. The memory required by the near matrix at 5 GHz is less than half of that required at 30 MHz. The memory required to store the ILU factorization is generally lower when the memory required by the near matrix is reduced.

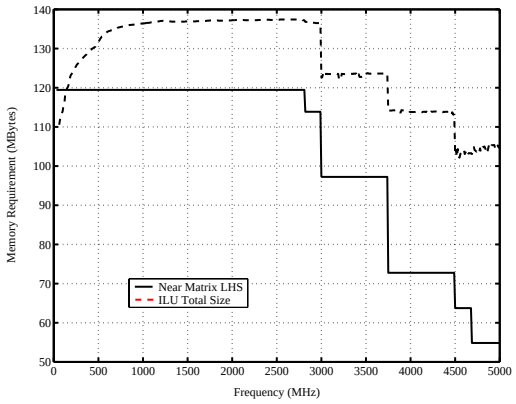

Figure 5. Memory cost of the near matrix and preconditioner.

To validate the EMAP5-FMM result, a cavity model was also used to calculate the input impedance of the same rectangular power bus structure. The cavity model has been widely used to analyze PCB power-return plane structures [20], [21]. For a thin power-return plane pair with a reasonably good dielectric and PEC conductors, the input impedance is approximately determined as,

$$Z_{in} = j\varpi\mu h \sum_{m=0}^{\infty}\sum_{n=0}^{\infty} \frac{\chi_{mn}^2 \cos^2\left(k_{xm}x_s\right)\cos^2\left(k_{yn}y_s\right)}{ab(k_{xm}^2 + k_{yn}^2 + \gamma^2)}. \tag{40}$$

A more detailed explanation of equation (40) can be found in [21]. Figure 6 compares the EMAP5-FMM result with the cavity model result. Although the cavity model does not account for the radiation from printed circuit board structures, there is good agreement between the two methods up to 5 GHz.

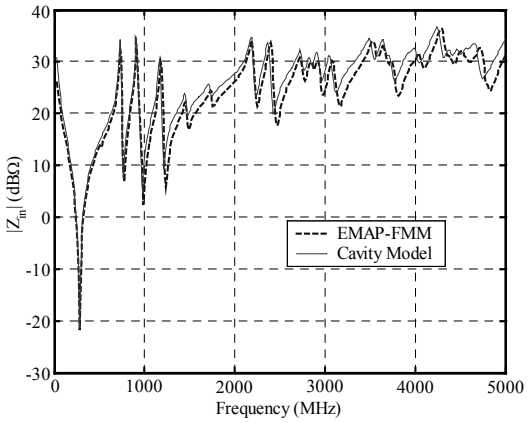

Figure 6. Input impedance comparison using EMAP5-FMM and cavity model.

The second sample problem is to calculate the bistatic radar cross section (RCS) of a perfectly conducting sphere. The radius of the sphere is 15 cm. The frequency of interest is 3 GHz. In this case, due to the large number of elements required, it is not possible to build a preconditioner from the matrix *LHS′* that fits in the physical memory of a personal computer. However, it is possible to construct an alternative preconditioner based on the FEM submatrix and an absorbing boundary condition (FEM-ABC) that is very memory efficient. In order to apply the ABC, the MoM boundary must be moved away from the PEC conductor and a specific CFIE form (TENH) is used [18]. An air sphere with a radius of 16 cm forms the MoM boundary, as shown in Fig. 7. More information on how to choose the location of the ABC can be found in [17].

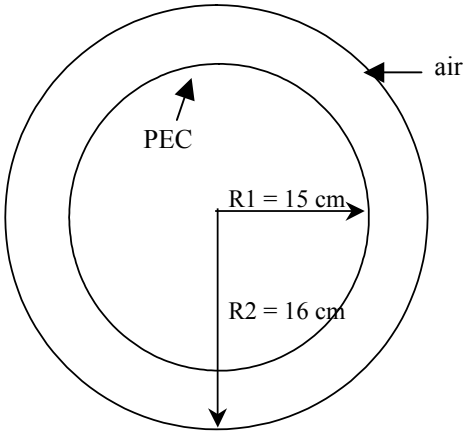

Figure 7. A perfectly conducting sphere.

Table 1 summarizes the discretization of this problem. The air layer generates 23,376 tetrahedral elements and 15,533 FEM inner edges. The triangular mesh density used for this problem is 10 elements per wavelength. If the MoM matrix is calculated directly using the MoM method, the memory requirement for the [*C*] and [*D*] matrices is about 6 GBytes, which greatly exceeds the physical memory of the personal computer used for this modeling.

Figure 8 illustrates the triangular surface mesh on the air sphere. There are a total of 194 groups on the surface. Ideally, groups on the surface of a symmetric structure like a sphere would have a similar number of elements. However, the grouping algorithm that we used produced several groups with only a few elements. A better grouping algorithm would balance the number of elements in each group. Nevertheless, the FMM algorithm performed very well for these examples.

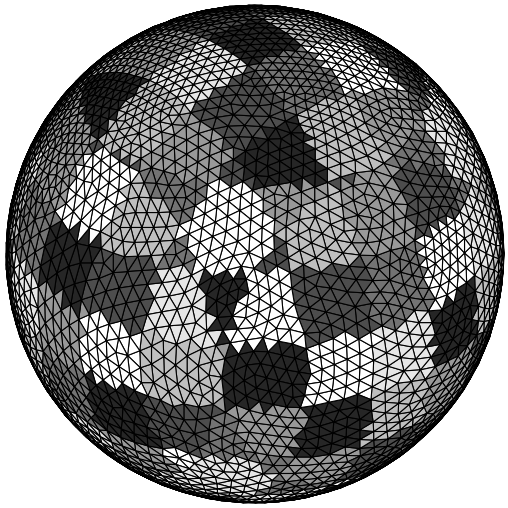

Figure 8. The meshes and groups for problem 2.

The memory required to store the near matrix *LHS′* in this case is about 1.2 GBytes, which is only *1/5* of that required to store the [*C*] and [*D*] matrices obtained by the MoM. However, this memory requirement is close to the limit of the personal computer used for this modeling. It is not possible to generate a precondtioner using ILU factorization of the near matrix *LHS′* on the same computer due to its huge memory requirement. Using a FEM-ABC preconditioner and techniques reported in [18], the memory required for the preconditioner is only about 0.02 GBytes and the BICGSTAB solution converges to a tolerance of 10^{-3} in 26 steps.

Analytical results for the RCS of this geometry can be obtained using the Mie series [22]. Figure 9 shows that the bistatic RCS results obtained using EMAP5-FMM agree with the Mie series results very well.

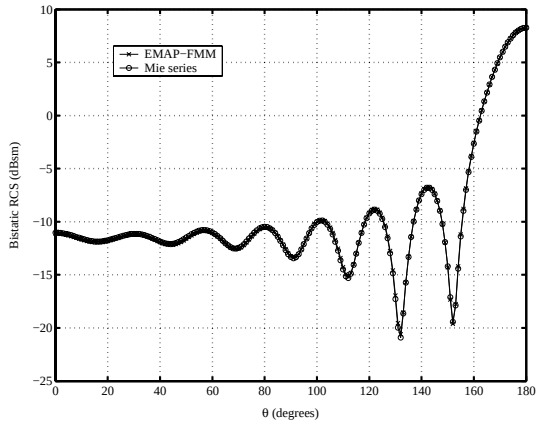

Figure 9. The bistatic RCS results of a perfect conducting sphere.

CONCLUSION

The fast multipole method was combined with a hybrid FEM/MoM method in this paper. Incorporating FMM allows an efficient evaluation of the surface integral and reduces the memory required to model structures with a large number of boundary elements. Two practical problems were investigated to validate the formulation and to demonstrate the memory efficiency of FMM. Good agreement was achieved between the FMM-enhanced hybrid FEM/MoM method and other analytical results.

For the first sample problem with 2,370 MoM boundary edges, the near matrix in the FMM employs about half of the memory required to store the fully-populated matrix generated by the MoM at 5 GHz. For the second sample problem with 13,779 MoM boundary edges, the near matrix uses about $1/5$ of the memory required to store the dense matrix generated by the MoM. If the FMM were applied to larger problems with more MoM boundary edges, we would expect even greater memory efficiency to be achieved.

Besides the near matrix, the preconditioner also usually requires a lot of memory in an iterative solver. Since the condition number of the matrices generated by the hybrid method is usually very large, the preconditioner is crucial for the efficient convergence of the iterative solver. A good preconditioner will reduce the required iterations dramatically and require very little memory and little time to construct. Without an effective preconditioner, the modeling of the second sample problem would have been much more difficult on a personal computer.

The FMM method implemented in this study does not work very well for electrically small structures due to the divergent nature of the spherical Hankel function used in this method. Electrically small structures that have many elements due to their geometric complexity are best modeled by locating the FEM/MoM boundary far from the complex part of the geometry. This minimizes the number of MoM boundary elements required and the total memory required to solve the problem.

The FMM method is designed to model electrically large structures with a large number of boundary elements. Its multilevel versions have been successfully employed to model structures such as aircraft with more than 10^7 boundary elements [11]. For electrically large geometries, a hybrid FEM/MoM technique incorporating FMM is capable of solving much larger problems in less memory than a standard FEM/MoM approach.

ACKNOWLEDGEMENT

The authors wish to express their thanks to Professor W. C. Chew of University of Illinois at Urbana-Champaign for providing the Mie series code.

REFERENCES

[1] V. Roklin, “Rapid solution of integral equations of scattering theory in two dimensions,” *J. Comput. Phys.*, vol. 86, pp. 414–439, Feb. 1990.

[2] N. Engheta, W.D. Murphy, V. Rokhlin and M.S. Vassiliou, “The fast multipole method for electromagnetic scattering problems,” *IEEE Trans. Antennas Propagat.*, vol. 40, no. 6, pp. 634–641, June 1992.

[3] N. Lu and J. Jin, “Application of fast multipole method to finite-element boundary-integral solution of scattering problems”, *IEEE Trans. Antennas Propagat.,* vol. 44, no. 6, pp. 781–786, June 1996.

[4] J. M. Song and W.C. Chew, “MLFMA for electromagnetic scattering from large complex objects,” *IEEE Trans. Antennas Propag.*, vol. 45, pp. 1488–1493, Oct. 1997.

[5] J. L. Volakis, T. Özdemir, and J. Gong, “Hybrid finite-element methodologies for antennas and scattering,” *IEEE Trans. Antennas Propagat.*, vol. 45, pp. 493–507, Mar. 1997.

[6] A. F. Peterson, S. L. Ray, and R. Mittra, *Computational Methods for Electromagnetics*, New York: IEEE Press and Oxford University Press, 1997.

[7] J. J. H. Wang, *Generalized Moment Methods in Electromagnetics*, New York: John Wiley & Sons, 1990.

[8] S. M. Rao, D. R. Wilton, and A. W. Glisson, "Electromagnetic scattering by surfaces of arbitrary shape," *IEEE Trans. Antennas Propagat.,* vol. 30, pp. 409–418, May 1982.

[9] X.-Q. Sheng, J.-M. Jin, J. Song, C.-C. Lu, and W.C. Chew, "On the formulation of hybrid finite-element and boundary-integral methods for 3-D scattering," *IEEE Trans. Antennas Propagat.*, vol. 46, pp. 303–311, Mar. 1998.

[10] Y. Ji, "Development and applications of a hybrid finite-element method/method-of-moments tool to model electromagnetic compatibility and signal integrity problems in printed circuit boards," Ph. D. dissertation, University of Missouri-Rolla, 2000.

[11] W. C. Chew, J.-M. Jin, E. Michielssen and J. Song, *Fast and Efficient Algorithms in Computational Electromagnetics*, Norwood, MA: Artech House Inc, 2001.

[12] R. Coifman, V. Roklin, and S. Wandzura, "The fast multipole method for the wave equation: a pedestrian prescription," *IEEE Antennas Propag. Mag.*, vol. 35, pp. 7–12, June 1993.

[13] Y. Ji, H. Wang and T. H. Hubing, "A novel preconditioning technique and comparison of three formulations for the hybrid FEM/MoM method," *Appl. Comput. Electromagn. Soc. (ACES) J.,* vol. 15, pp. 103–114, July 2000.

[14] J. M. Song and W.C. Chew, "Fast multipole method solution using parametric geometry," *Micro. Opt. Tech. Lett.*, vol. 7, pp. 760–765, Nov. 1994.

[15] Y. Saad, *Iterative Methods for Sparse Linear Systems*, Boston: PWS Publishing Company, 1996.

[16] A. Heldring, J. M. Rius and L. Ligthart, "New block ILU preconditioner scheme for numerical analysis of very large electromagnetic problems," *IEEE Trans. Magn.*, vol. 38, no. 2, pp. 337–340, Mar. 2002.

[17] J. Liu and J.-M. Jin, "A highly effective preconditioner for solving the finite element-boundary integral matrix equation of 3-D scattering," *IEEE Trans. Antennas Propagat.*, vol. 50, no. 9, pp. 1212–1221, Sep. 2002.

[18] C. Guo and T. H. Hubing, "Effective preconditioners for the solution of hybrid FEM/MoM matrix equations using combined formulations", submitted to *Appl. Computat. Electromagn. Soc. (ACES) J.*

[19] Y. Ji and T. H. Hubing, "EMAP5: A 3D hybrid FEM/MoM code," *Appl. Computat. Electromagn. Soc. (ACES) J.*, vol. 15, pp. 1–12, Mar. 2000.

[20] Y. T. Lo, D. Solomon, and W. F. Richards, "Theory and experiment on microstrip antennas," *IEEE Trans. Antennas Propagat.*, vol. 27, no. 2, pp. 137–145, March 1979.

[21] M. Xu and T. Hubing, "Estimating the power bus impedance of printed circuit boards with embedded capacitance," *IEEE Trans. Adv. Packag.*, vol. 25, no. 3, pp. 424–432, Aug. 2002.

[22] W. C. Chew, *Waves and Fields in Inhomogeneous Media*, New York: IEEE Press, 1995.

Chunlie Guo earned his BSEE and MSEE degrees from Tsinghua University in 1998 and 2000, respectively. He is currently pursuing a Ph.D. degree in Electrical Engineering at the University of Missouri-Rolla. His graduate research is focused on the development of numerical modeling techniques for analyzing signal integrity and electromagnetic compatibility problems.

Todd Hubing received his BSEE degree from MIT in 1980, his MSEE degree from Purdue University in 1982, and his Ph.D. in Electrical Engineering from North Carolina State University in 1988.

From 1982 to 1989, he was an electromagnetic compatibility engineer for IBM in Research Triangle Park, NC. He is currently a Professor of Electrical and Computer Engineering at the University of Missouri-Rolla. He serves on the Board of Directors and is a Past President of the IEEE EMC Society.